Optical crosstalk in interdigitated lateral PIN photodiodes

P. S. MENON, B. BAIS[a], AIMI AZRI MOHD JHI[a], S. SHAARI
Photonics Technology Laboratory (PTL) Institute of Micro Engineering and Nanoelectronics (IMEN),
[a]Department of Electrical, Electronics and System Engineering, Faculty of Engineering and Built Environment, Universiti Kebangsaan Malaysia 43600 UKM, Bangi, Selangor, Malaysia

This paper presents an investigation of the optical crosstalk in lateral interdigitated PIN photodiodes (ILPP) with top illumination. Three different substrates were used; silicon, germanium and indium gallium arsenide. Device parameters that were evaluated were the doping concentration in the p+ and n+ wells, the absorption layer thickness and the distance between the electrodes on each one of these substrates. From the evaluation of 27 types of ILPP, it was discovered that the absorption layer thickness of 1 μm on an InGaAs substrate has the lowest crosstalk value of -143.65 dB. Usage of numerical evaluation prior to actual device fabrication reduces device fabrication cost and time as well as provides an insight into the physics of the device which may not be executable in the actual fabricated device.

(Received April 3, 2012; accepted June 6, 2012)

Keywords: Interdigitated, Photodiode, Crosstalk, Numerical modeling, Lateral, p-i-n

1. Introduction

A PIN photodiode (PD) is the most commonly employed light detector in today's fiber optic communications systems because of its ease of fabrication, high reliability, low noise, low voltage and relatively high bandwidth [1-2]. In particular, the interdigitated lateral PIN photodiode (ILPP) can be fabricated using complementary-metal-oxide semiconductor (CMOS) techniques such as diffusion and/or ion implantation [3].

In the past, the ILPP structure has been developed on many different substrates utilizing different materials as the absorbing layer depending on the respective wavelengths. These include silicon [4], silicon-on-SOI (silicon-on-insulator) [5], Ge-on-SOI [6], GaAs [7] and InGaAs [8-11]. The structures developed on InGaAs/InP substrates have exhibited a -3dB frequency of 2 GHz (λ=1.54 μm), 7.5 GHz (λ=1.3 μm), 560 MHz (λ=1.3 μm) and 100 MHz (λ=1.55 μm), respectively. The devices achieved quantum efficiencies/responsivities of 45%, 95% (0.53 A/W), 0.56 A/W and 0.2 A/W, respectively. Silicon-based photodiodes are normally used in the visible spectrum (0.4 μm -1.1 μm) whereas Ge-based and InGaAs-based photodiodes are utilized in the infra-red spectrum which is up to 1.55 μm.

Optical crosstalk arises when the incident light on one channel is coupled to another channel (usually the adjacent one) by reflection or poor fiber coupling to photodetector or by lateral diffusion of optically generated carriers. By virtue of the illumination technique and array geometry, it can be assumed that optical crosstalk is due to lateral diffusion of photogenerated carriers [12]. Crosstalk is important as it increases the device noise and affects the detection sensitivity. Previous work showed a 10% (-20 dBm) optical crosstalk on a 2D back-illuminated, silicon vertical pin photodiode array with 16x16 elements device with pixel pitch of 1 mm, gap size of 200 μm and absorption layer thickness of 50 μm [13]. The 4 channel InGaAs-based vertical pin photodiode array device developed by Shirai et. al [14] with 250 μm pitch produced an optical crosstalk of -35dB (1.77%) and was improved to -40 dB (1%) with the inclusion of trenches between adjacent channels.

This paper presents an investigation of optical crosstalk evaluation on the design of ILPP using an industrial-based numerical software [15]. The ILPP design was adopted from previous research work [16-17]. To the best of our knowledge, a comparison in optical crosstalk between different substrate materials and device parameters has only been performed in this work [18].

2. Theory and modeling

The modeling of the ILPP was performed using a commercial numerical simulator which utilizes a drift-diffusion approach [14]. The Poisson, carrier continuity and current density equations are solved numerically in three dimensions subject to the device's geometry and boundary conditions imposed by the device's contacts and biasing conditions. Three-dimensional simulation package SILVACO ATLAS was used to model the ILPP which takes into account the following physical models; concentration-dependent minority carrier lifetime model, concentration and temperature-dependent mobility model, parallel field mobility, Shockley-Read-Hall (SRH) recombination model, Auger recombination model, optical generation/radiative recombination model and Fermi-Dirac statistics.

Crosstalk in an ILPP occurs due to the free carriers that are generated in the intrinsic region of the basic p-i-n anode-cathode unit. Instead of being collected by the p-i-n unit where it was generated, the free carrier is absorbed and collected by the adjacent or neighbouring anode-cathode pair. The design parameters of an ILPP such as the distance between the electrodes, the thickness of the absorption layer and the junction doping concentration are factors that could affect the crosstalk value. Besides that, different substrate materials also affect the crosstalk value. Fig. 1 illustrates the phenomenon of crosstalk in the ILPP.

Firstly, an optical source is provided to only one pair of the anode-cathode electrodes in the interdigitated photodiode where the common cathode is biased with a certain voltage. In the ILPP device presented in Fig. 1 with 5 pairs of electrodes, optical illumination is present between Anode_3 and Cathode. Subsequently, the generated photocurrent at every other anode-cathode electrode pair is extracted.

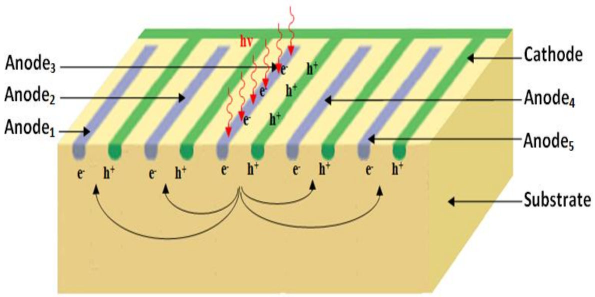

Fig. 1. Crosstalk phenomenon in ILPP.

Therefore, the crosstalk at Anode_1 for ILPP in Fig. 1 is given by:

$$Crosstalk = 20 * log\left(\frac{I_{Anode1}}{I_{Anode3}}\right) \tag{1}$$

where $I_{Anode,n}$ is the photocurrent that flows at $Anode_n$ where n is *1, 2, 3* and so on.

The total crosstalk for any ILPP is the total sum of photocurrent at $Anode_n$ (excluding the Anode that was illuminated with optical light) over the photocurrent generated at the illuminated Anode. Hence, the total crosstalk of ILPP in Fig. 1 is given by:

$$\text{Total\_Crosstalk} = 20\log\left(\frac{I_{\text{Anode1}} + I_{\text{Anode2}} + I_{\text{Anode4}} + I_{\text{Anode5}}}{I_{\text{Anode3}}}\right) \tag{2}$$

where $I_{Anode,n}$ is the photocurrent that flows at $Anode_n$ where n is *1, 2, 3* and so on.

3. Results

Fig. 2 shows the three dimensional view of the ILPP with 10 pairs of anode-cathode electrodes where optical illumination is present in only one pair of the electrodes (Anode_5). Optical illumination is 10 mW/cm^2 and bias voltage of the common cathode is 5 V. The total width of the device is 52 μm and the length is 50 μm. Fig. 3(a) and Fig. 3(b) portrays the cross sectional view of the device for the p+ and n+ doping, respectively. Three different substrate materials, namely silicon, germanium and InGaAs were used as the absorption layer. For each one of these substrates, the distance between the electrodes, the junction doping concentration and the absorption layer thickness were varied and the effect of these variations on the crosstalk value were analyzed. Table 1 lists the differences in material parameters for the three substrates.

Table 1. Material parameters for the different substrates.

Parameter	Silicon	Germanium	$In_{0.53}Ga_{0.47}As$
Energy Gap, E_g (eV)	1.08	0.66	0.734
Electron mobility, μ_n ($cm^2V^{-1}s^{-1}$)	1000	3900	3372
Hole Mobility, μ_p ($cm^2V^{-1}s^{-1}$)	500	1900	75
Electron Lifetime τ_n (ns)	100	10	0.7
Hole Lifetime, τ_p (ns)	100	10	31
Optical wavelength (μm)	1.0	1.4	1.55

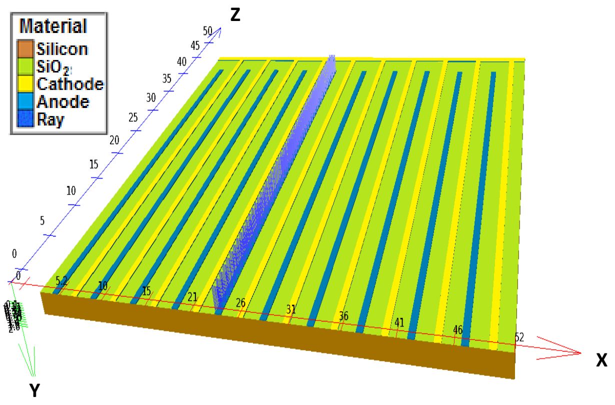

Fig. 2. Three dimensional view of ILPP with optical illumination on one pair of electrodes.

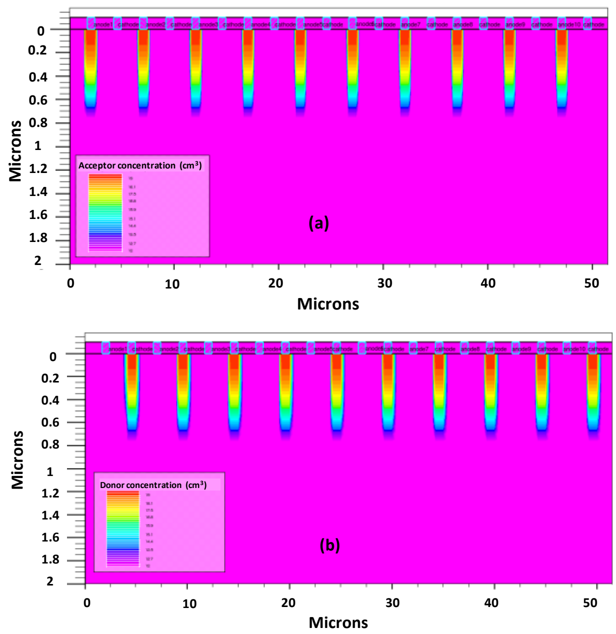

Fig. 3. Two dimensional cross sectional view of (a) p+ doping and (b) n+ doping within the ILPP.

Fig. 4 displays the effect of the distance between electrodes to the total crosstalk. Three different distances were selected i.e. 0.5 µm, 1.0 µm and 1.5 µm. From Fig. 4, it is seen that, as the distance between electrodes were increased, the total crosstalk decreases for all substrates. This is because the longer the distance, the probability that the generated electron and hole pairs (e-h) within the illuminated electrode, to diffuse to adjacent electrodes reduces. The highest crosstalk of -12 dB (25.1%) was produced in Ge-based ILPPs whereas the lowest crosstalk of -42 dB (0.79%) was recorded for a Si substrate with distance between electrodes of 1.5 µm. However, larger electrode distances decreases the speed of the device. Therefore, there is a tradeoff between the switching speed and the crosstalk.

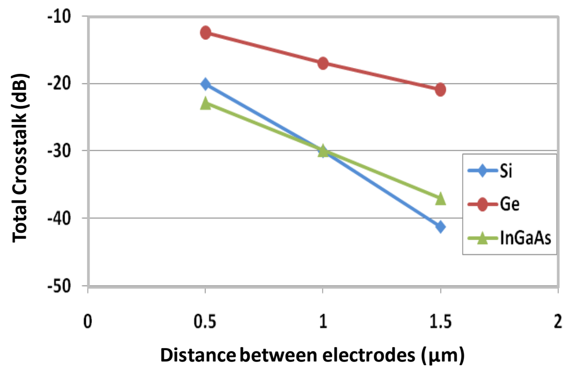

Fig. 4. Total crosstalk for distance between electrodes.

Fig. 5 shows the effect of junction doping concentration on the total crosstalk where the doping concentration was varied for three different values i.e. 10^{17} cm^{-3}, 10^{18} cm^{-3}, 10^{19} cm^{-3}. For all substrates, a similar trend is observed where as the doping concentration is increased, the total crosstalk decreases. A higher doping concentration produces higher electric field between the illuminated electrode pair. The probability of generated e-h to be collected by adjacent electrodes reduces drastically. The highest crosstalk of -21 dB (8.9%) was produced in a germanium-based ILPP device whereas the lowest crosstalk of -45 dB (0.56%) was produced by an ILPP device using InGaAs as the absorption layer with a junction doping concentration of 1e19 cm^{-3}.

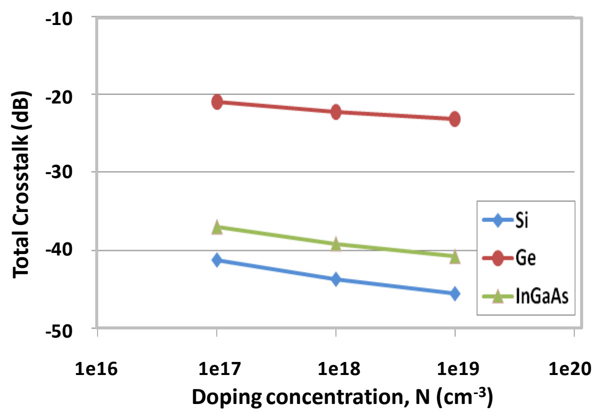

Fig. 5. Total crosstalk for various junction doping concentration.

The effect of total crosstalk due to the absorption layer thickness is given in Fig. 6. The absorption layer thickness was varied between 1 µm, 2 µm and 3 µm. A similar trend is observed in all substrates where as the absorption layer thickness is increased, the total crosstalk increases as well. This is because for a given junction depth in the ILPP, a shorter substrate absorption thickness decreases the probability of e-h diffusion to adjacent electrode pair. For a thicker absorption layer, e-h can be generated deeper within the substrate and they are prone to diffuse to the adjacent electrodes hence increasing the total crosstalk. It is also observed that the absorption layer thickness has the most profound effect on the total crosstalk as compared to the other factors analyzed in this work. The highest crosstalk of -21 dB (8.9%) was recorded for a Ge-based ILPP with absorption layer thickness of 3 μm whereas the lowest crosstalk of -143 dB (~0%) was extracted for an InGaAs-based ILPP with 1 μm absorption layer. In terms of speed, a thinner absorption layer is preferred but at the expense of a reduced device efficiency.

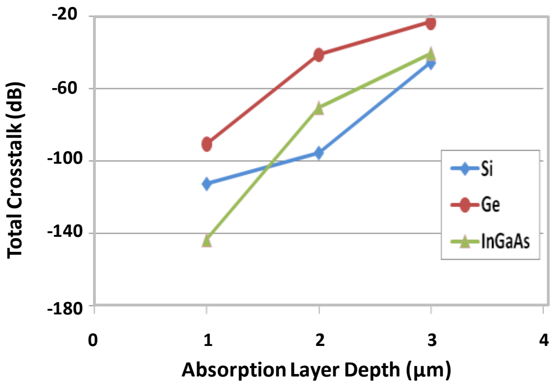

Fig. 6. Total crosstalk versus absorption layer depth.

4. Conclusion

We have demonstrated and analyzed the effect of ILPP design parameters on the total crosstalk within the device. Substrate material, distance between electrodes, junction doping concentration and absorption layer thickness were varied and the total crosstalk was extracted and compared. Total crosstalk increases when the distance between electrodes and absorption layer thickness is small but crosstalk decreases for high doping concentrations. Substrate materials with low electron lifetime such as InGaAs show lower crosstalk values compared to other substarte materials. As a conclusion, the lowest crosstalk of -143.63 dB within an ILPP device can be achieved using an InGaAs-based ILPP with distance between electrodes of 1.5 μm, p+ and n+ doping concentration of 10^{19} cm^{-3} and absorption layer thickness of 1 μm where the optical crosstalk is almost negligible.

Acknowledgement

The authors would like to acknowledge the support of Universiti Kebangsaan Malaysia for funding this work under grants UKM-OUP-NBT-27-119/2011 and UKM-GGPM-NBT-090-2010.

References

[1] D. J. Jackson, D. L Persechini, Tech. Dig. Topical Meeting Opt. Fiber Comm., New Orleans, 100 (1986).
[2] S. N. Subbarao, D. W. Bechtle, R. J. Menna, J. C. Connolly, R. L. Camisa, S. Yegnanarayan, IEEE Trans. Microw. Theory Tech., **38**, 1199 (1990).
[3] P. S. Menon, K. Kandiah, S. Shaari, Proc. IEEE Int. Conf. Semicon. Elec., art no. 4266614, 276 (2006).
[4] C. L. Schow, R. Li, J. D. Schaub, J. C. Campbell, IEEE J. Quantum Electron., **35**, 1478 (1999).
[5] R. Li, J. D. Schaub, S. M. Csutak, J. C. Campbell, IEEE Photon. Technol. Lett., **12**, 1046 (2000).
[6] S. J. Koester, J. D. Schaub, G. Dehlinger, J. O. Chu, IEEE J. Quantum Electron., **12**, 1489-1502 (2006).
[7] W. Giziewicz, S. Prasad, C. J. Fonstad Jr, Proc. IEEE on Sensors; **1**, 284 (2004).
[8] N. Yasouka, T. Sanada, H. Hamaguchi, M. Makiuchi, T. Mikawa, A. Kuramata, O. Wada, R. J. Deri, IEEE Electron. Lett., **27**, 2020 (1991).
[9] S. Tiwari, J. Burroughes, M. S. Milshtein, M. A. Tischler, S. L. Wright, IEEE Photon. Technol. Lett., **4**, 396 (1992).
[10] W. S. Lee, S. A. Kitching, S. W. Bland, IEEE Electron. Lett., **25**, 522 (1989).
[11] T. W. Jeong, K. Iiyama, S. Takamiya, Proc. Int. Conf. InP Rel. Mater., 250-253 (2005).
[12] M.-L. Hsia, Z. M. Liu, C. N. Chan, O. T –C Chen. Proc. IEEE on Sensors, 1689 (2011).
[13] I. Goushcha, I., B. Tabbert, A. O. Goushcha. IEEE Nuclear Sci. Symp. Conf. Record, **6**, 4348 (2007).
[14] T. Shirai, M. Minamino, T. Higuchi, M. Iwase, OFC 2001, **3**, 2001, p. WDD73 - WDD73.
[15] SILVACO Int., ATLAS User's Manual. 10th ed.; Sunnyvale, CA, (2010).
[16] P. S. Menon, K. Kandiah, A. A. Ehsan, S. Shaari, Int. J. Num. Model.: Electron. Netw. Dev. Fields **24**(5), 465 (2011).
[17] P. S. Menon, K. Kandiah, A. A. Ehsan, S. Shaari, Proc. of SPIE 6838, 2008, art. no. 68380C.
[18] Aimi Azri Mohd Jhi. Disertasi Sarjana Muda, Universiti Kebangsaan Malaysia. (2010).

*Corresponding author: susi@eng.ukm.my